applied sciences

MDPI

Article

Calibrated Hydraulic Resistance Adjuncts for Carbon Dioxide Angiography Optimization

Ivan Corazza [1,*], Pier Luca Rossi [2] and Romano Zannoli [1]

[1] Medical Physics Activities Coordination Centre, Department of Medical and Surgical Sciences (DIMEC), Alma Mater Studiorum University of Bologna, 40138 Bologna, Italy
[2] Occupational Safety and Health Service, Alma Mater Studiorum University of Bologna, 40127 Bologna, Italy
* Correspondence: ivan.corazza@unibo.it

Abstract: Background: Despite the growing interest in CO_2 angiography, some mechanical aspects related to CO_2 injection still need to be deepened, and some improvements are still possible. This work explores the possibility of optimizing gas injection into small-sized arteries. Since the image quality depends on how the gas fills the vessel and is strongly dependent on injection flow, the possibility of controlling the flow is mandatory to obtain good results. To better control the flow, we propose to adjunct small tubes with known hydraulic resistances in parallel to the injection catheter, allowing the generation of the desired injection flow by modulating the injection pressure. Methods: Using a mechanical mock of the cardiovascular system, we measured pressures and flows of interest and acquired the optical images of the vessel during gas injections. We performed a simulation with four different calibrated adjunct resistances in various injection pressure conditions, with and without saline flushing. Results: Our tests demonstrated that the optimized injection of the gas maintains the same procedure durations and reduces the gas volume and the local pressure increase, avoiding the local gas "explosion" in the injection site. Conclusions: Our proposal appears effective and paves the way for research into optimizing clinical CO_2 angiography procedures.

Keywords: carbon dioxide angiography; injection line hydraulic resistance; bubble shapes; bubble distribution; injection flow; procedure optimization

Citation: Corazza, I.; Rossi, P.L.; Zannoli, R. Calibrated Hydraulic Resistance Adjuncts for Carbon Dioxide Angiography Optimization. *Appl. Sci.* **2024**, *14*, 1276. https://doi.org/10.3390/app14031276

Received: 23 November 2023
Revised: 29 January 2024
Accepted: 1 February 2024
Published: 3 February 2024

Correction Statement: This article has been republished with a minor change. The change does not affect the scientific content of the article and further details are available within the backmatter of the website version of this article.

1. Introduction

Carbon dioxide angiography [1] is experiencing significant growth thanks to the placing on the market of injectors capable of controlling all injection parameters and radiological equipment with dedicated protocols [2,3].

Many of the clinical innovations were born in laboratories and operating rooms. An accurate bench-based evaluation of what happens in biomechanical terms for optimizing procedures has rarely been carried out in-depth, and some aspects can be improved [4–6].

Nowadays, automatic constant pressure CO_2 injectors permit the setting of the optimal gas input flow (mL/s) in a vascular cavity to obtain good radiological imaging with acceptable patient discomfort [2,7–10].

CO_2 angiography differs from traditional angiography with an iodinated contrast medium for three main reasons: (1) The iodinated contrast medium mixes with the blood, while the CO_2 displaces and replaces it. (2) Gas bubbles behave differently depending on the vessel's size and blood flow. (3) CO_2 injection catheters have very low hydraulic resistance, reducing the possibility of controlling gas injection by acting on pressure, which has an impact on imaging quality. To optimize CO_2 imaging, it is essential to know the behavior of the injected gas bubbles within the bloodstream and, therefore, to change the injection mode depending on the site where the CO_2 is being injected. We can consider three cases: huge cavities, medium-sized arteries and veins, and small diameter vessels (<6 mm).

In all biomechanical conditions, to have a good radiological image, the easiest way is to fill the blood vessel with gas as much as possible so that CO_2 replaces the blood in the portion of interest. However, the blood moves with pulsatile pressure and flow, complicating the procedure. As far as large arteries are concerned [11–13], it is necessary to inject a large amount of gas to fill the cavity as much as possible, and this is carried out using high injection pressures, generating pain and discomfort for the patient [14–16]. For arteries and veins with a diameter greater than 6 mm, imaging optimization occurs mainly by optimizing the gas injection flow according to the blood flow in the vessel [5]. In the case of small blood vessels (diameter < 6 mm), the gas bubbles fill their entire lumen. If the injection gas flow is lower than blood flow, the vessel fills partially and presents areas with gas alternating with regions of blood flowing along the duct. In this case, if the subtraction angiography is not performed correctly, there is a risk of a suboptimal visualization of the area of interest. Suppose large quantities of gas are injected, and gas flow overcomes the blood flow. In that case, reflux can push the blood backward to the large arteries with a local increase in pressure at the injection site and possible pain for the patient (with consequent movements and artifacts on final images).

The optimal solution is to control the injection flow better, setting it slightly lower than blood flow. However, this is very difficult to achieve because, with catheters with low hydraulic resistance, minor variations in pressure due to vascular pulsatility are sufficient to modify what happens inside the blood vessel.

The clinician knows that the instantaneous gas input flow ($F_g(t)$, mL/s) [17] corresponds to the instantaneous difference between the injector pressure (P_{inj}) and the internal vascular cavity pressure (P_{int}), divided by the hydraulic resistance (R_{es}) of the injection line (Hagen–Poiseuille's Law [18]):

$$F_g(t) = \frac{P_{inj} - P_{int}(t)}{Res} \ ([mL/s]) \quad (1)$$

This formula shows how difficult it is to control the gas injection efficiently by acting only on the injection pressure because vascular cavity pressure pulsates, and the catheter used for diagnostic and interventional approaches has its hydraulic resistance (from 2 mmHg/(mL/s) up to 100 mmHg/(mL/s)) [5].

The problem is particularly evident in the case of low blood flow or small vessels with physiological pulsatile pressure (femoral arteries, foot arteries, and subclavian arteries). In these conditions, to have a desired low gas flow injection using catheters with internal channel suitable for a standard wire guide (0.035 in = 0.889 mm) and consequent low resistance (~5 mmHg/(mL/s)), it would be necessary to use injection pressure, only slightly higher than vascular one, with an instantaneous gas injection strongly dependent from the patient pressure pulsatility. Moreover, since the blood flow is pulsatile and in phase with the pressure, the result is a minimum gas injection flow corresponding to the maximum instantaneous blood flow, precisely the opposite of what is desired for optimal angiographic imaging.

A possible solution to this problem is to use thinner catheters with higher resistance and pressure but with unaffordable procedural issues. A possible alternative is to use usual (low hydraulic resistance) catheters and connections, with standard wire guides and good maneuverability, with an adjunct appropriate calibrated hydraulic resistance tube (R_{adj}) in series. This trick allows the gas input flow ($F_g(t)$) to be more easily controlled and stabilized. A higher injection pressure (P_{inj}) must be used without changing the standard diagnostic procedure and devices to compensate for the adjunct resistance effect on gas flow. To avoid an increased procedural complexity, the calibrated hydraulic resistance adjunct may be mounted in parallel with a low resistance stopcock to permit an easy passage from a high gas flow rate, used in large vascular cavities, to a low gas flow rate, used in small vascular vessels, without changing the injection line and catheter (Figure 1). This solution makes the gas injection rate more regular, especially in wide pulse arterial pressure cases. Gas bubbles are more regularly injected and distributed inside the vessel, with consequent possible

imaging benefits. A higher hydraulic resistance also permits easier control of gaseous retrograde flow in the vessel, reducing the patient's pain.

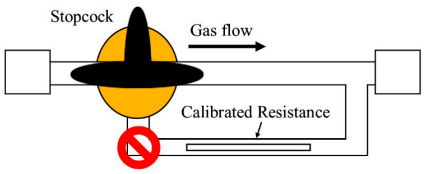

(a) Bypassed calibrated resistance

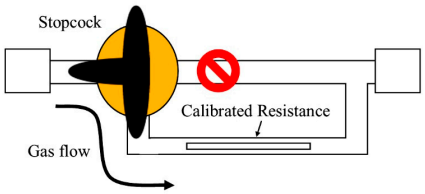

(b) Adjunct calibrated resistance inserted

Figure 1. System to change the hydraulic resistance: (**a**) the stopcock allows the flow directly to the catheter, avoiding adjunct resistance; (**b**) the gas flows in the adjunct resistance and then the injection catheter.

We tested this approach on a vascular simulator with transparent vessels to visually observe the effect of the adjunct resistances and also to clarify if it is better for imaging to have inside the target vessel many regularly distributed running bubbles obtained by an adjunct resistance device and higher injection pressure, or small volumes of gas fulfilled vascular sections followed by gas empty ones, obtained without adjunct resistance and low-pressure injection. Moreover, the records can clarify how the injection time courses (gas output delay and duration) change with and without resistance adjunct.

Maybe other questions will arise from our results; they will be discussed and described in subsequent simulations and testing.

2. Materials and Methods

2.1. Experimental Setup

For this research, 3 calibrated hydraulic resistance adjuncts have been assembled using different lengths of low internal diameter tubes (2F endovascular catheters) (Figure 2). The tube length ranged between 32 cm and 55 cm. The hydraulic resistances of the standard injection line (R_{line}) and the adjuncts (R_{adj}) have been experimentally evaluated by recording the exponential pressure decay of a known volume CO_2-filled chamber; the complete measurement method is described in a previous paper [19].

The apparatus described in Figure 3 has been used to simulate the CO_2 angiographic process. The alternating pump (simulating the left ventricle) pushes a colored saline solution (blood) into the aorta through the aortic valve. The blood flows into the arterial tree and then into the venous system. From here, blood enters the atrium and then, through the mitral valve, to the ventricle. By regulating the stopcocks, it was possible to set the peripheral resistance and, therefore, the mean arterial pressure. Pulse pressure was settled by modulating the compliance of the aorta [20].

A pressure transducer (Edwards TruWave, Edwards Lifesciences Corp, Irvine, CA, USA) connected to a Dash 3000 acquisition unit (GE HealthCare, Chicago, IL, USA) and an electromagnetic flowmeter (Biotronex 610 square wave EMF, Biotronex Laboratory Inc, Silver Spring, MD, USA) were used to acquire the internal arterial pressure (P_{int}) and flow ($F_a(t)$). A settable frame rate digital TV camera (model acA 1300-75gc, Basler, Ahrensburg, Germany) interfaced with a Matrox Concord Card (Matrox, Dorval, QC, Canada) allowed to record videos of blood flow and bubble motion during the procedures. Arterial pressure,

aortic flow, and video output were acquired simultaneously with the ANScovery system (Sparkbio Srl, Bologna, Italy) [21].

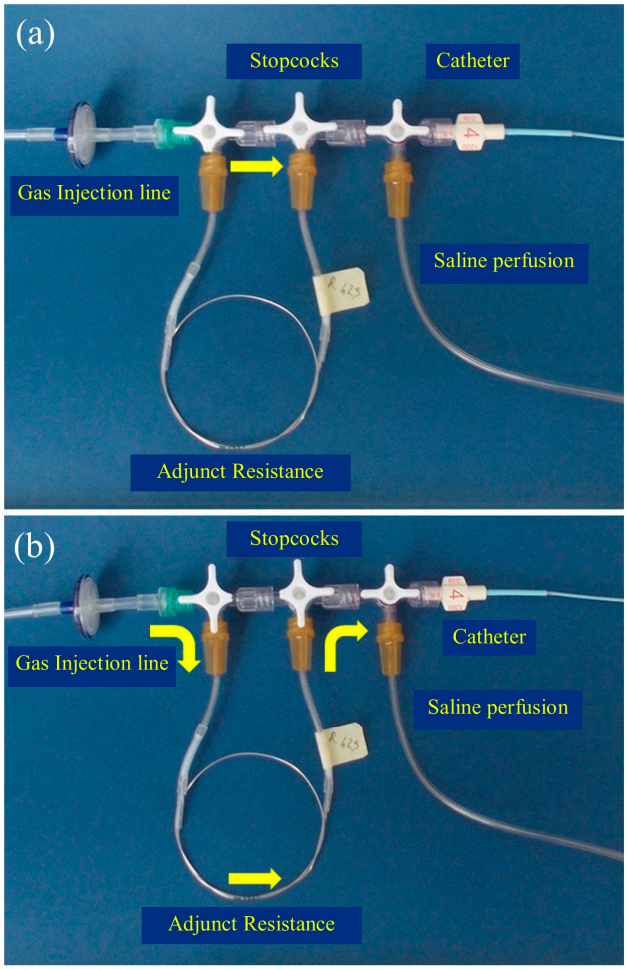

Figure 2. Variable hydraulic resistance for two different conditions: (**a**) without any external adjunct resistance; (**b**) with the calibrated adjunct resistance.

An automatic CO_2 injector (Angiodroid Srl, Bologna, Italy) was used to inject fixed gas volumes (V_{inj}) at constant pressures (P_{inj}) inside the arterial tree through a standard gas injection line (mod CO200001, Angiodroid Srl, Bologna, Italy) with a 5F Cordis catheter (Cordis, Milpitas, CA, USA). Two 3-ways stopcocks at the beginning of the injection catheter permitted the insertion of the calibrated hydraulic resistance adjuncts (Figure 2).

Signal analysis and imaging evaluation were performed with the ANScovery software (version 8.0).

The target vessel network image is shown in Figure 4.

The measured hydraulic resistance adjuncts' values were 28 mmHg/mL/s, 42 mmHg /mL/s, and 69 mmHg/mL/s, respectively. The hydraulic resistance (R_{line}) of the standard gas injection line, connections, and stopcocks was 5.5 mmHg/mL/s (1 mmHg/mL/s = $1.33 \cdot 10^8$ N·s·m^{-5}).

So, 4 different conditions have been simulated, considering that the total resistance for each condition is given by summing R_{line} to R_{adj}: (a) no adjunct resistance (only R_{line}); (b) R_{line} + 28 mmHg/mL/s; (c) R_{line} + 42 mmHg/mL/s; and (d) R_{line} + 69 mmHg/mL/s.

The pulsatile behavior of the vascular simulator was set to produce 2 mL stroke volume each second in the target vessel, with a vascular pressure pulse of 150/80 mmHg (mean value 120 mmHg) and peak flow of 3.8 mL/s. The instantaneous flow signal was recorded before the injection point to avoid the noise of bubble passage through the electromagnetic probe. In all the subsequent measurements, an injection volume of 20 mL was set, and the

gas injection image was continuously observed and recorded from the pressure onset to the last injected bubble. For each adjunct resistance, the gas injection pressure has been calculated from Hagen–Poiseuille's Law (Equation (1)) to obtain, in the target vessel in correspondence with the peak pressure (P_{int}(max)), a gas inflow equal to the mean saline flow (2.0 mL/s):

$$P_{inj} = P_{int}(max) + R_{adj} \cdot 2.0 \text{ mL/s} \quad (2)$$

The injection pressures (P_{inj}) resulted, respectively, 150 mmHg for no R_{adj} (without the adjunct resistance); 206 mmHg for R_{adj} = 28 mmHg/mL/s; 234 mmHg for R_{adj} = 42 mmHg/mL/s; and 288 mmHg for R_{adj} = 69 mmHg/mL/s.

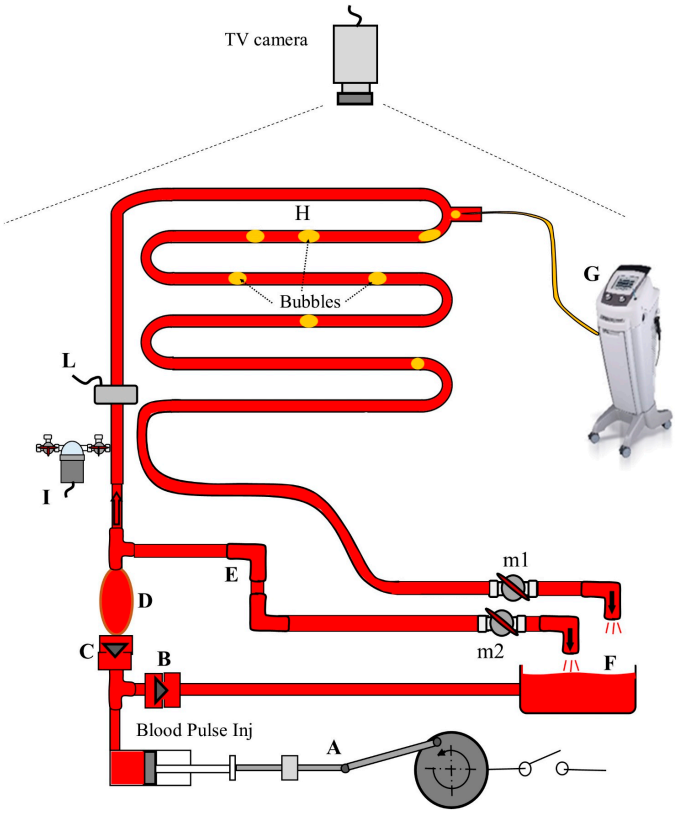

Figure 3. Apparatus to simulate CO_2 angiographic process: (A) syringe-like pump generates pulsatile pressures and flows; (B) mitral valve; (C) aortic valve; (D) aorta; (E) venous return system; (F) atrium; (G) gas injector with injection pressure (P_{inj}) and volume (Vinj) control; (H) arterial glass tree (diameter 6 mm) for CO_2 injection; (I) pressure transducer to measure arterial pressure (P_{int}); (L) electromagnetic flowmeter to measure arterial flow (F_a(t)); (m1 and m2) stopcocks.

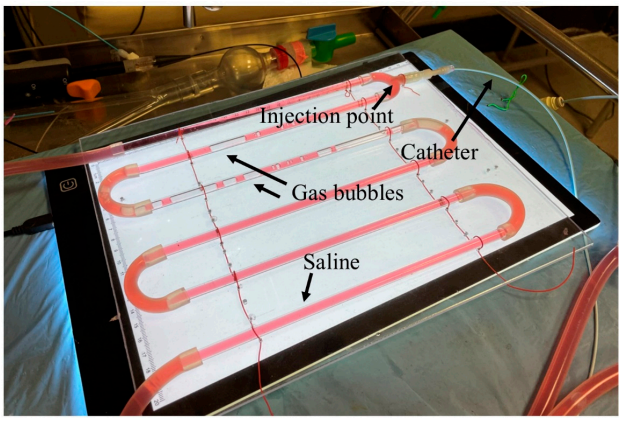

Figure 4. Vessels' network used for CO_2 injection.

2.2. Experimental Procedures

The pulsatile condition started activating the motor. After stabilization, the gas injection (20 mL) was performed (with gas flushing [13,22] of 1 mL), and pressures, flow, and bubble sequence captured by the camera were continuously monitored. The process has been repeated with only the standard line and the three resistance adjuncts. Each condition (with and without R_{adj}) was tested with the calculated injection pressures.

Then, injections were repeated with a saline-filled catheter to simulate operative conditions with a perfused catheter [23]. The saline was added with blue-colored ink to observe the process of catheter emptying and liquid and gas passage. The injection with blue saline was repeated only for 2 different conditions: (a) P_{inj} = 150 mmHg, no adjunct resistance; (b) P_{inj} = 288 mmHg and R_{adj} = 69 mmHg/mL/s.

Recorded frames were converted to grayscale for each described condition to simulate "radiological images". Before starting the CO_2 injection, the last frame was used as a mask to be subtracted from the subsequent frames to highlight the bubbles. Then, the masked frames were stacked to obtain the full image of the inner vessel [24].

Then, the subsequent parameters were measured and compared: (a) time to obtain the full radiological image of the vessel; (b) delay between pressure onset and gas output; (c) gas volume injection duration; (d) arterial pressure increase during injection; and (d) length of the backward vessel filling in case of gas reflux.

3. Results

Figure 5 shows a frame for each injection condition, extracted 2 s and 4 s after starting gas injection. It is possible to see the bubbles' dimensions: Without resistances, the bubbles are bigger and tend to fulfill the vessel with an extended retrograde flow. With different resistance adjunct values, bubbles are smaller and move along the vessel with a lower retrograde flow.

Despite the different effects on the bubbles' dimensions and distribution without and with adjunct resistances, the final masked and stacked images are very similar (Figure 6), and the only difference is in the length of the vessel highlighted by the gas reflux.

Table 1 shows the injection durations, the times necessary to obtain the same complete final radiological image, and the "size" of the reflux, quantified as the length of the tube covered by the backward gas flow in the gas-flushed catheter condition.

Systolic and diastolic arterial pressure increases for each condition are shown in Table 2.

The results of the comparison of delays between pressure onset and gas output and injection duration for the 2 conditions with blue saline are shown in Table 3.

Table 1. Injection durations for each condition.

Injection Pressure (mmHg)	R_{adj} (mmHg/mL/s)	Duration ± 0.4 (s)	Time to Obtain the Complete Radiological Image ± 0.4 (s)	Tube Length Covered by Reflux (cm)
150	0	10.5	8.0	2
206	0	6.0	7.8	>24
	28	10.4	7.8	6
234	0	4.1	7.8	>24
	42	7.5	8.0	8
288	0	4.0	7.7	>24
	69	7.5	8.3	7

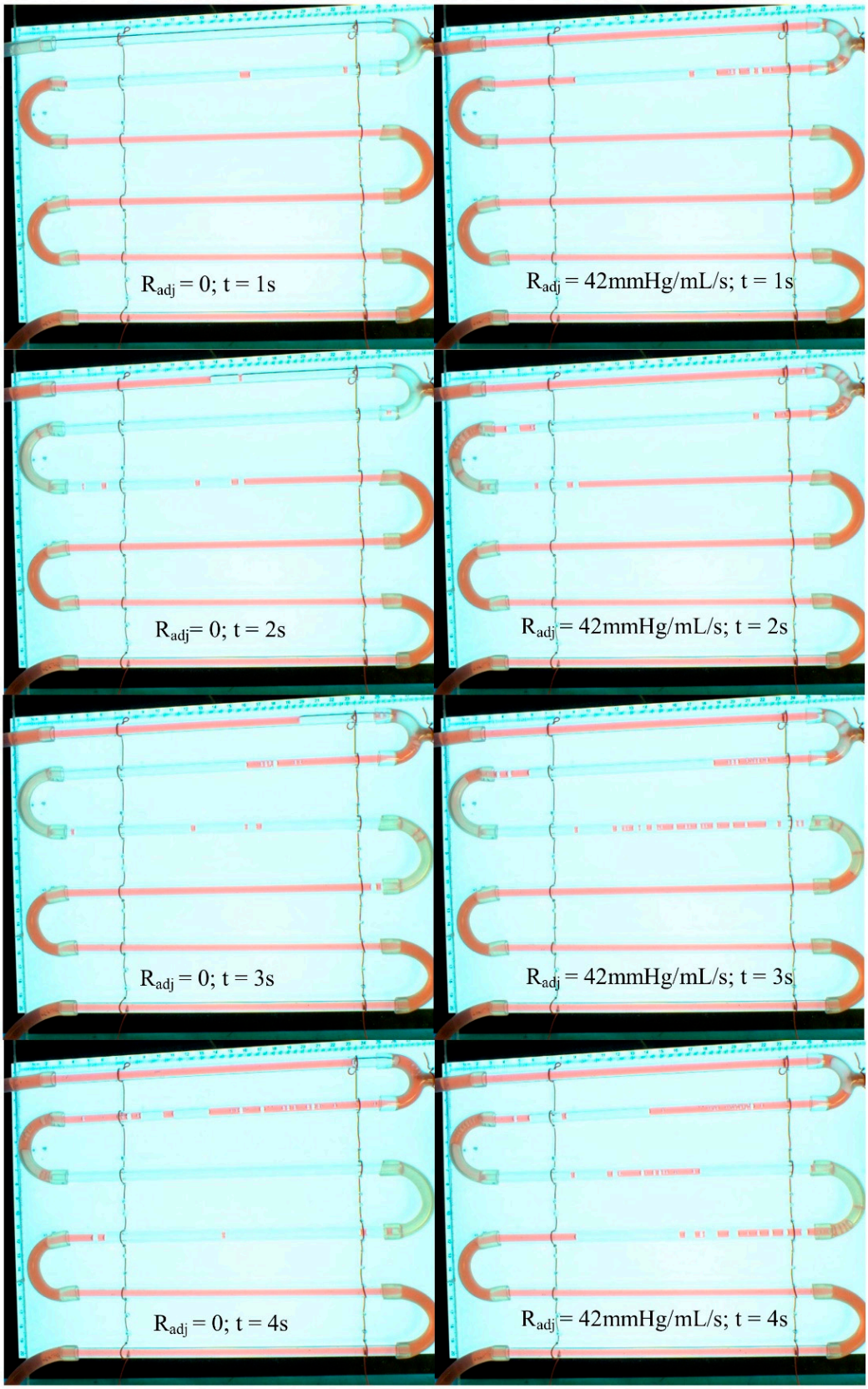

Figure 5. Example of bubble dimension and spatial distribution with an injection pressure of 234 mmHg without R_{adj} and with R_{adj} = 42 mmHg/mL/s, at 1 s, 2 s, 3 s, and 4 s after gas injection start.

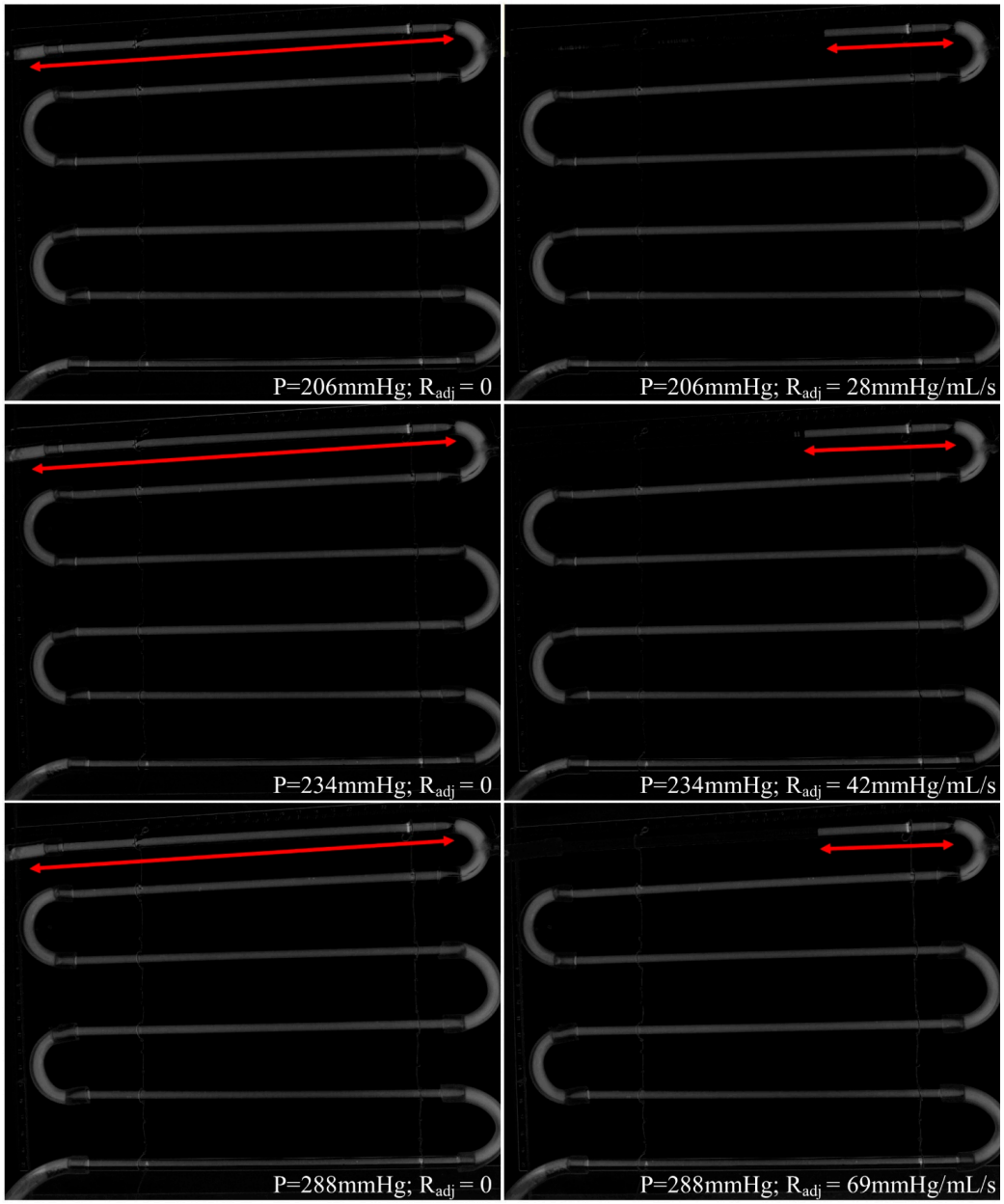

Figure 6. Stacked images for three conditions (P_{inj} = 206 mmHg, R_{adj} = 0, R_{adj} = 28 mmHg/mL/s; P_{inj} = 234 mmHg, R_{adj} = 0, R_{adj} = 42 mmHg/mL/s; P_{inj} = 288 mmHg, R_{adj} = 0, R_{adj} = 69 mmHg/mL/s). Red arrows indicate the reflux.

Table 2. Maximum pressure increases during injection at different conditions.

Injection Pressure (mmHg)	R_{adj} (mmHg/mL/s)	Systolic Increase after Injection ± 2 (mmHg)	Diastolic Increase after Injection ± 2 (mmHg)
150	0	7	5
206	0	10	25
	28	6	10
234	0	13	25
	42	6	10
288	0	15	25
	69	10	10

Table 3. Values of injection delays between pressure onset and gas output for 2 simulated conditions.

		Catheter with Saline
P_{inj} (mmHg)	R_{adj} (mmHg/mL/s)	Delay ± 0.4 (s)
150	*0*	6.0
288	*69*	7.0

4. Discussion

It is well known that the image quality of CO_2 angiography is limited by the low contrast of the gas, and the operators try to inject as much gas as possible in the shortest time to fulfill the target vascular cavities. The hydraulic resistance of the injection line has been seen as the main limitation to obtaining a rapid filling of large vascular cavities, and some tricks have been suggested to overcome it. Why do we suggest increasing the injection line resistance by inserting an adjunct tube in series? By using new automatic gas injectors [13,25] with settable injection pressure, it has been demonstrated that in small diameter vessels (leg arteries), using standard catheters, the best imaging is obtained with low injection pressure, slightly higher than the maximum arterial value [2]. Unfortunately, this setting has the drawback of arterial pressure pulsatility, which hardly modulates the gas injection in an undesirable way. In fact, the gas input flow results are high when the blood flow is low, producing a nonregular vascular gas filling with gas-filled vascular sectors followed by gas-empty ones. A solution to compensate for the effect of the physiological pulsatility is to increase the injection pressure, increasing the hydraulic resistance of the line to maintain the gas inflow at the desired value. With this solution, the gas bubble sequence changes towards a more regular distribution and possibly better imaging. This solution is convenient only for small vessels where a low gas inflow is required. The gas injection flow must be very high for large cavities and vessels with high blood flow, and no resistance adjunct is permitted. This separation of radiological targets with different procedural approaches is not easily understood by clinicians, especially if unusual physics concepts are involved. For this reason, we simulated the clinical context and produced "visible" evidence of the expected benefits. Apart from the methods used to build the resistance adjuncts and to measure the resistance values for CO_2 gas fluid, this approach permits putting the CO_2 angiographic procedure in a more rigorous scientific frame, where the operator can move quantitatively to the desired results. For CO_2 angiography, described as a highly operator-dependent procedure, the possibility to control each step represents a revolution. This revolution can be possible only thanks to the availability of settable pressure and volume automatic injectors and a more precise biomechanical description. This paper focused our analysis on medium-sized arterial vessels (iliac/femoral arteries). Still, the same process can be moved to smaller arterial vessels (pedidial arteries) and some venous applications (arteriovenous artificial fistula, transcatheter chemoembolization, etc.) with a significant possibility to improve the diagnostic and therapeutic results by optimizing the gas injection process.

Regarding the results of this paper, the most important one is the correspondence between what was obtained and visually observed and what was calculated and desired. It was a pleasure to observe how the different resistance adjuncts modify the bubbles' shapes and sequence and how the different sequences may produce useful diagnostic images, with contrast gas saving, lower local pressure increases (mean increases of 7 mmHg vs. 13 mmHg for systolic and 10 mmHg vs. 25 mmHg for diastolic pressures), and the same time interval to produce a complete image of the considered district (time differences: 0 s for P_{inj} = 206 mmHg; 0.2 s for P_{inj} = 234 mmH; and 0.6 s for P_{inj} = 288 mmHg). The injections without Radj produced significant reflux (>24 cm) and bigger bubbles compared to what happened with the adjunct resistances (reflux of about 6 cm).

Moreover, the delays between injection start and gas output with saline-filled catheters are comparable (6 s and 7 s). This last evidence seems incomprehensible: higher line resistance, same gas output delay! This effect is due to the increased applied pressure value

to compensate for the increased line resistance. Immediately after the pressure onset, the whole injection system is described as a series of two hydraulic resistances: the first of the thin gas-filled adjunct and the second of the catheter filled with saline. Initially, this second resistance shows a higher value due to the high viscosity of the liquid and progressively decreases during catheter purging. During the purging phase, lasting from the injection pressure onset, the fluid flow from the catheter hole is mainly controlled by the catheter hydraulic resistance and the driving pressure ($P_{inj} - P_{vasc}$). With the driving pressure higher to compensate for the adjunct, the purging interval is shorter. This evidence opens a new possibility: by using resistance adjuncts, it is possible to avoid catheter gas purging before CO_2 diagnostic injection, which may be a significant procedural benefit!

We tested the effect of the resistance adjuncts on a simulator and not directly on patients because these devices, also simple, are not jet-suitable on the market, and we had to use different hand-made prototypes that were laboratory-calibrated. However, the transition to the clinical procedure is not as complex as one might believe because it is sufficient to know the hydraulic resistances of the catheters usually used in clinical practice and use them to build the additional resistances required.

Also, using these adjuncts opens exciting perspectives on the imaging side. We have a better distribution of the injected bubbles in the target vascular field, but we do not know how the imaging system manages this. With this solution, different frame rates and frame intervals may play a better role. Moreover, the optimized injection of the gas reduces the gas volume and the local pressure increase, avoiding the local gas "explosion" in the injection site [24] with benefits for patient pain reduction, representing an open issue. In most scientific papers about CO_2 angiography, percentages of adverse events are always reported (more frequently, pain, nausea, or vomiting) [22,26,27]. These events are generally related to the increase in local pressure at the injection site, the occlusion of the vessel under investigation, and any anterior peripheral vascular branches occluded by reflux. Moreover, pain may induce patients to move during gas injection, affecting the imaging technique, introducing artifacts [28], and requiring restarting the procedure with additional time-consuming and increased radiological doses. Additional resistances reduce the local increase in blood pressure and reflux and so can reduce pain; their possible benefits are evident.

5. Conclusions

In summary, the proposal of hydraulic resistance adjuncts opens many research (physical and clinical) windows on future CO_2 angiography scenarios since it allows better control of carbon dioxide injection flow, which is mandatory to optimize the clinical procedures, with no effect on the quality of the final images. Moreover, a lower pressure increase and a reduced retrograde gas flow can be associated with lower patient pain, with evident benefits for the procedure. An adequate clinical trial is necessary.

Author Contributions: Conceptualization, I.C. and R.Z.; Methodology, I.C. and P.L.R.; Software: I.C.; Validation, I.C., R.Z. and P.L.R.; Writing—Original Draft Preparation, I.C.; Writing—Review and Editing: I.C., R.Z. and P.L.R. All authors have read and agreed to the published version of the manuscript.

Funding: This research received no external funding.

Institutional Review Board Statement: Not applicable.

Informed Consent Statement: Not applicable.

Data Availability Statement: Data are available on request to the corresponding author.

Conflicts of Interest: The authors declare no conflicts of interest.

References

1. Hawkins, I.F.; Caridi, J.G. Carbon Dioxide (CO_2) Digital Subtraction Angiography: 26-Year Experience at the University of Florida. *Eur. Radiol.* **1998**, *8*, 391–402. [CrossRef]
2. Palena, L.M.; Diaz-Sandoval, L.J.; Candeo, A.; Brigato, C.; Sultato, E.; Manzi, M. Automated Carbon Dioxide Angiography for the Evaluation and Endovascular Treatment of Diabetic Patients with Critical Limb Ischemia. *J. Endovasc. Ther.* **2016**, *23*, 40–48. [CrossRef]
3. Fontana, F.; Piacentino, F.; Ossola, C.; Curti, M.; Coppola, A.; Carcano, G.; Piffaretti, G.; Tozzi, M.; Venturini, M. Successful Endovascular Management with a Covered Stent of an External Iliac Pseudoaneurysm Following Allograft Nephrectomy Using CO2 as Contrast Medium: A Case Report. *Radiol. Case Rep.* **2021**, *16*, 3821–3823. [CrossRef] [PubMed]
4. Ali, M.; Noureldin, M.; Kashef, O.E.; Zaghlol, H. Safety and Effectiveness of Carbon Dioxide Contrast Medium in Infra-Inguinal Endovascular Interventions for Patients With Chronic Threatening Lower Limb Ischemia and Renal Impairment: A Multicentric Trial. *J. Endovasc. Ther.* **2023**, *16*, 15266028231159241. [CrossRef] [PubMed]
5. Corazza, I.; Sapignoli, S.; Cercenelli, L.; Marcelli, E.; Faggioli, G.; Gargiulo, M.; Stella, A.; Diemberger, I.; Rossi, P.L.; Zannoli, R. Automated CO2 Angiography: Injection Pressure and Volume Settings. *Med. Eng. Phys.* **2020**, *80*, 65–71. [CrossRef] [PubMed]
6. Vacirca, A.; Faggioli, G.; Mascoli, C.; Gallitto, E.; Pini, R.; Spath, P.; Logiacco, A.; Palermo, S.; Gargiulo, M. CO_2 Automated Angiography in Endovascular Aortic Repair Preserves Renal Function to a Greater Extent Compared with Iodinated Contrast Medium. Analysis of Technical and Anatomical Details. *Ann. Vasc. Surg.* **2022**, *81*, 79–88. [CrossRef] [PubMed]
7. Kroneberger, C.; Enzweiler, C.N.; Schmidt-Lucke, A.; Rückert, R.-I.; Teichgräber, U.; Franiel, T. Contrast-Induced Nephropathy in Patients with Chronic Kidney Disease and Peripheral Arterial Disease. *Acta Radiol. Open* **2015**, *4*, 2058460115583034. [CrossRef] [PubMed]
8. Mehran, R.; Nikolsky, E. Contrast-Induced Nephropathy: Definition, Epidemiology, and Patients at Risk. *Kidney Int. Suppl.* **2006**, *100*, S11–S15. [CrossRef] [PubMed]
9. Giordano, A.; Messina, S.; Polimeno, M.; Corcione, N.; Ferraro, P.; Biondi-Zoccai, G.; Giordano, G. Peripheral Diagnostic and Interventional Procedures Using an Automated Injection System for Carbon Dioxide (CO_2): Case Series and Learning Curve. *Heart Lung Vessel.* **2015**, *7*, 18–26. [PubMed]
10. Bürckenmeyer, F.; Schmidt, A.; Diamantis, I.; Lehmann, T.; Malouhi, A.; Franiel, T.; Zanow, J.; Teichgräber, U.K.M.; Aschenbach, R. Image Quality and Safety of Automated Carbon Dioxide Digital Subtraction Angiography in Femoropopliteal Lesions: Results from a Randomized Single-Center Study. *Eur. J. Radiol.* **2021**, *135*, 109476. [CrossRef]
11. Gallitto, E.; Faggioli, G.; Vacirca, A.; Pini, R.; Mascoli, C.; Fenelli, C.; Logiacco, A.; Abualhin, M.; Gargiulo, M. The Benefit of Combined Carbon Dioxide Automated Angiography and Fusion Imaging in Preserving Perioperative Renal Function in Fenestrated Endografting. *J. Vasc. Surg.* **2020**, *72*, 1906–1916. [CrossRef]
12. Mascoli, C.; Faggioli, G.; Gallitto, E.; Vento, V.; Indelicato, G.; Pini, R.; Vacirca, A.; Stella, A.; Gargiulo, M. The Assessment of Carbon Dioxide Automated Angiography in Type II Endoleaks Detection: Comparison with Contrast-Enhanced Ultrasound. *Contrast Media Mol. Imaging* **2018**, *2018*, 7647165. [CrossRef] [PubMed]
13. Mascoli, C.; Faggioli, G.; Gallitto, E.; Vento, V.; Pini, R.; Vacirca, A.; Indelicato, G.; Gargiulo, M.; Stella, A. Standardization of a Carbon Dioxide Automated System for Endovascular Aortic Aneurysm Repair. *Ann. Vasc. Surg.* **2018**, *51*, 160–169. [CrossRef] [PubMed]
14. Criado, E.; Upchurch, G.R.; Young, K.; Rectenwald, J.E.; Coleman, D.M.; Eliason, J.L.; Escobar, G.A. Endovascular Aortic Aneurysm Repair with Carbon Dioxide-Guided Angiography in Patients with Renal Insufficiency. *J. Vasc. Surg.* **2012**, *55*, 1570–1575. [CrossRef] [PubMed]
15. Fujihara, M.; Kawasaki, D.; Shintani, Y.; Fukunaga, M.; Nakama, T.; Koshida, R.; Higashimori, A.; Yokoi, Y.; CO2 Angiography Registry Investigators. Endovascular Therapy by CO2 Angiography to Prevent Contrast-Induced Nephropathy in Patients with Chronic Kidney Disease: A Prospective Multicenter Trial of CO2 Angiography Registry. *Catheter. Cardiovasc. Interv.* **2015**, *85*, 870–877. [CrossRef] [PubMed]
16. De Angelis, C.; Sardanelli, F.; Perego, M.; Alì, M.; Casilli, F.; Inglese, L.; Mauri, G. Carbon Dioxide (CO2) Angiography as an Option for Endovascular Abdominal Aortic Aneurysm Repair (EVAR) in Patients with Chronic Kidney Disease (CKD). *Int. J. Cardiovasc. Imaging* **2017**, *33*, 1655–1662. [CrossRef] [PubMed]
17. Chanson, H. 13—Summary of Basic Hydraulic Principles. In *Hydraulics of Open Channel Flow, 2nd*; Chanson, H., Ed.; Butterworth-Heinemann: Oxford, UK, 2004; pp. 249–252. ISBN 978-0-7506-5978-9.
18. Pfitzner, J. Poiseuille and His Law. *Anaesthesia* **1976**, *31*, 273–275. [CrossRef] [PubMed]
19. Corazza, I.; Taglieri, N.; Pirazzini, E.; Rossi, P.L.; Lombi, A.; Scalise, F.; Caridi, J.G.; Zannoli, R. Carbon Dioxide Coronary Angiography: A Mechanical Feasibility Study with a Cardiovascular Simulator. *AIP Adv.* **2018**, *8*, 015225. [CrossRef]
20. Zannoli, R.; Corazza, I.; Branzi, A. Mechanical Simulator of the Cardiovascular System. *Phys. Medica* **2009**, *25*, 94–100. [CrossRef]
21. Corazza, I.; Barletta, G.; Guaraldi, P.; Cecere, A.; Calandra-Buonaura, G.; Altini, E.; Zannoli, R.; Cortelli, P. A New Integrated Instrumental Approach to Autonomic Nervous System Assessment. *Comput. Methods Programs Biomed.* **2014**, *117*, 267–276. [CrossRef]
22. Thomas, R.P.; Viniol, S.; König, A.M.; Portig, I.; Swaid, Z.; Mahnken, A.H. Feasibility and Safety of Automated CO_2 Angiography in Peripheral Arterial Interventions. *Medicine* **2021**, *100*, e24254. [CrossRef] [PubMed]

23. Caridi, J.G.; Hawkins, I.F.; Klioze, S.D.; LeVeen, R.F. Carbon Dioxide Digital Subtraction Angiography: The Practical Approach. *Tech. Vasc. Interv. Radiol.* **2001**, *4*, 57–65. [CrossRef] [PubMed]
24. Cho, K.J.; Hawkins, I.F. *Carbon Dioxide Angiography Principles, Techniques, and Practices*; Informa Healthcare: New York, NY, USA, 2007; ISBN 978-1-4200-1626-0.
25. Massaini, G.; Lazzarotto, T.; Masciello, F.; Panci, S.; Michelagnoli, S.; Chisci, E. A Pilot Study of Endovascular Repair for Ruptured Aortic Aneurysms with the Use of Carbon Dioxide Angiography Alone. *J. Endovasc. Ther.* 2023, *ahead of print*. [CrossRef] [PubMed]
26. Wagner, G.; Glechner, A.; Persad, E.; Klerings, I.; Gartlehner, G.; Moertl, D.; Steiner, S. Risk of Contrast-Associated Acute Kidney Injury in Patients Undergoing Peripheral Angiography with Carbon Dioxide Compared to Iodine-Containing Contrast Agents: A Systematic Review and Meta-Analysis. *J. Clin. Med.* **2022**, *11*, 7203. [CrossRef]
27. Liss, P.; Eklöf, H.; Hellberg, O.; Hägg, A.; Boström-Ardin, A.; Löfberg, A.-M.; Olsson, U.; Örndahl, P.; Nilsson, H.; Hansell, P.; et al. Renal Effects of CO_2 and Iodinated Contrast Media in Patients Undergoing Renovascular Intervention: A Prospective, Randomized Study. *J. Vasc. Interv. Radiol.* **2005**, *16*, 57–65. [CrossRef]
28. Sharafuddin, M.J.; Marjan, A.E. Current Status of Carbon Dioxide Angiography. *J. Vasc. Surg.* **2017**, *66*, 618–637. [CrossRef]